УДК 621.317

AC BRIDGES WITH PHASE CONTROLLED DIVIDERS-THEORY AND EXPERIMENTAL RESULTS (МОСТЫ ПЕРЕМЕННОГО ТОКА С ФАЗОВЫМ УПРАВЛЕНИЕМ – ТЕОРИЯ И РЕЗУЛЬТАТЫ ЭКСПЕРИМЕНТА)

M.N. Surdu, *doctor of science, professor, leading scientist of Institute of electrodynamics of National Academy on Science of Ukraine, Kiev*

D.M. Surdu, *postgraduate student of Politechnical Institute, Lvov*

М.Н. Сурду

Д.М. Сурду

Описывается новый метод построения делителей напряжения с высокорасчетным эквивалентным коэффициентом деления, основанный на синтезе напряжения с регулируемым модулем посредством сложения напряжений с цифровой регулировкой фазы. Рассматриваются примеры построения прецизионных универсальных мостов, построенных с применением предложенного метода. Исследуется вариационный способ уравновешивания моста с фазовым управлением и сравнением токов. Предложены и исследованы методы вариационной коррекции погрешности измерения в таких мостах. Приведены результаты экспериментальных исследований.

The new approach to the creation of the equivalent voltage dividers is proposed. This approach is based on the synthesis of the sinusoidal signal with controlled magnitude by the algebraic summing of the signals, having digitally controlled phase. The universal wide range bridge was developed on this base. The variation method of the uncertainty correction in such bridges was proposed and developed. The bridge properties were analyzed and experimentally investigated.

Introduction

For the precise impedance measurements on audio frequency range main laboratories usually use simple [1–9] or quadrature [10–14] transformer bridges. Such bridges contain, as main part, some (2–6 or more) precision transformer dividers. It leads to big dimensions, narrow frequency range and high cost of the devices. These disadvantages sharply increase on the lower frequencies and make impossible creation of the transformer bridge for very low frequencies. This is the reason why replacing of the inductive divider in impedance measurements by another device could be very useful.

The digital synthesis of the signals and creation on this basis of different bridges has been widely used recently [15–24]. But these bridges can't compete in accuracy with transformer bridges.

So, the main problem consists of the following: most accurate transformer bridges have excellent accuracy, but big dimensions and cost makes it difficult to operate in low frequency range.

Solution – simple main idea

The fig. 1 on the plane of complex numbers (1, j.) shows basic signal (vector U_0), which coincide with real axis and two additional vectors U_{11} and U_{21}. The bisectrix divides onto two angle between vectors U_{11} and U_{21}. It is turned relatively real axis on the angle φ.

Additional and basic signals (vectors U_0, U_{11} and U_{21}) could have different magnitudes and phases (Ψ_{11} and $-\Psi_{21}$) but it is preferable to use the signals, satisfying to the equality:

$$|U_0| = |U_{11}| = |U_{21}|; \quad \Psi_{11} = -\Psi_{21}. \qquad (1)$$

Let's sum additional vectors U_{11} and U_{21}. The total balancing vector U_1^+ lies on the bisectrix.

Equation (2) describes this signal:

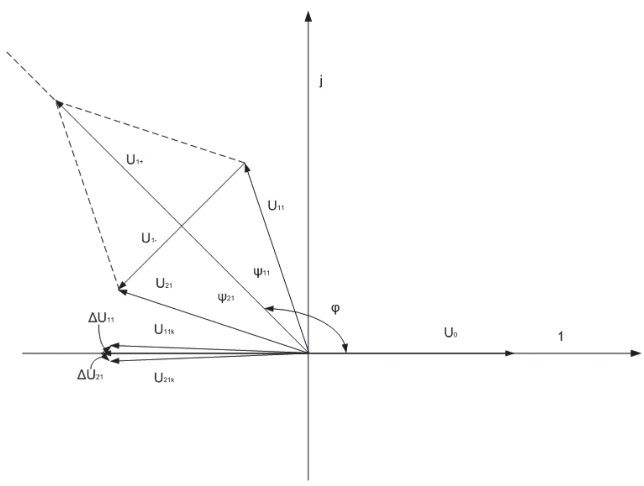

Fig. 1. Phase control vector diagram

$$U_1^+ = 2|U_0|\cos\psi \cdot \sin(\omega t + \varphi) = \rho_c e^{-j\varphi}. \quad (2)$$

Let's subtract additional vectors U_{11} and U_{21}. The differential balancing vector U_1^- is perpendicular to the bisectrix. Next equation describes this signal:

$$U_1^- = 2|U_0|\sin\psi \cdot \sin(\omega t + \varphi) = \rho_s e^{-j(\varphi+\pi/2)}. \quad (3)$$

Let's change the angles ψ_{11} and ψ_{21} simultaneously from zero to the same current value $|\psi|$. From the equations (2) and (3) we see that in both these cases we can change the magnitude of the balancing signal U_1 by controlling of the phases ψ_{11} and ψ_{21} only. The magnitude of the signal U_1 can be changed in the range of 0 to $\pm 2U_0$. Its phase can be changed in the range of 0 to ±180°.

Using the signals U_0 and U_1 we can create universal balanced bridges for measurements of any type of impedances. Such bridge will be balanced by changing of the signals phases only. This approach was proposed in [25–27].

The dependence of the vector U_1 magnitude on the phase angle ψ is nonlinear. It doesn't influence on the measurement accuracy because of this dependence is precisely calculated. But the derivative of this dependence changes in whole range of angle ψ of 0 to 1. The zero value of the derivative could create difficulties in the balancing process of the automated bridge. If we will limit the range of the vector U_1 changing, for example, to the maximal value $|U_1| \leq \sqrt{2}|U_0|$, the derivative will change in the range of 0,5 to 1 only. Such change of the derivative (and appropriate bridge sensitivity) doesn't influence on the balancing process. It only slightly (on $\sqrt{2}$) restricts the range of measurement.

Described above system of vectors isn't unique, which permits to create the balancing vector, controlled in magnitude by phase control. It is simplest one only. The calibration procedure of the bridges which uses this system is the simplest as well.

Signals U_0, U_{11} and U_{21} could be easily created using modern digital technique – by synthesis circuit (synthesizers). This technique was developed, for example, in [15,16]. Many authors describe the bridges, based on synthesizers [17–24].

Synthesizer's transfer coefficient in audio frequency range has rather big uncertainty – usually around 10^{-4} or worse. But these synthesizers could have rather good short term (during one measurement – one minute or less) stability.

Let's determine and eliminate the initial difference of the vectors U_{11}/U_0, and U_{21}/U_0 ratios from the nominal value. In this case only short term instability of these ratios and accuracy of the vectors U_{11} and U_{21} phase changing will influence on the common uncertainty of measurement.

Using proper components and structures, temperature stabilization, etc. we can reduce synthesizer short term (during 1 minute or less) instability to value of 10^{-8} or less.

Accuracy of the phase changing is limited by synthesizer phase noise only. On audio frequencies, this value can be lower than 10^{-9}.

A lot of different bridges could be created using described approach.

Bridge balance procedure

Let's consider the simplest bridge with current comparison, based on the phase control. Bridge consists of three synthesizers – S_0, S_{11} and S_{21}, which are supplied by standard DC source $U_=$. Synthesizers generate the sinusoidal voltages U_0, U_{11} and U_{21}. The adder Σ sums the voltages U_{11} and U_{21} and creates the balancing voltage U_1.

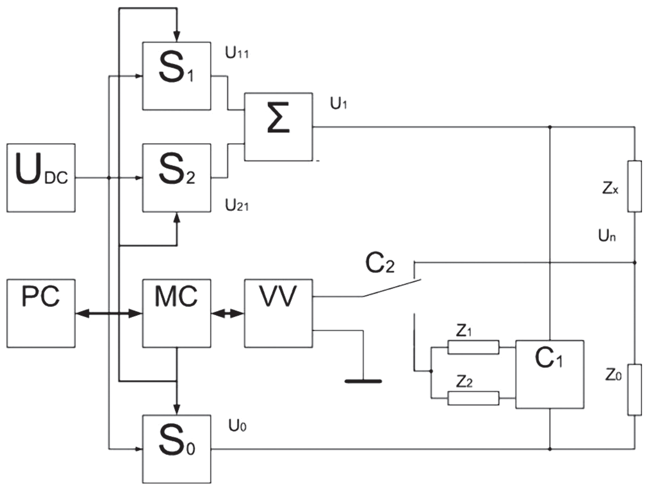

Fig. 2. High impedance bridge with phase controlled balance

The high potential ports of the standards being compared, Z_x and Z_0, are connected to voltage U_1 and U_0 sources. Low potential ports of these standards are connected together and through the switcher C_2, to the input of the vector voltmeter VV. Last one measures bridge unbalance signal and transfers results of measurements to the microcontroller MC (or PC). MC and PC processes results of VV measurement and balances the bridge by appropriate algorithm. MC also controls the operation of all synthesizers.

Equation (3) describes the balance condition of the bridge:

$$\frac{Z_x}{Z_0} = \frac{U_{1b}}{U_{0b}}, \quad (4)$$

where U_{1b} and U_{0b} are the values of the voltages U_1 and U_0 in the point of the bridge balance.

Let's balance the bridge, changing the magnitude and the phase φ of the vector U_1. In this case the equation (4) can be rewritten in the form:

$$\frac{z_x}{z_0} = \frac{U_{1b}}{U_{0b}} = (2\cos\psi_b)\cdot e^{-j\varphi b}, \quad (5)$$

where ψ_b and φ_b are the phases of the appropriate signals in the point of the bridge balance.

Equation (5) shows that we can get direct reading, if we will describe ratios $\frac{Z_x}{Z_0}$ and $\frac{U_{1b}}{U_{0b}}$ as follow:

$$\frac{Z_x}{Z_0} = \rho_x e^{-j\varphi_x} \text{ and } \frac{U_{1b}}{U_{0b}} = \rho_b e^{-j\varphi_b}.$$

In this case the balancing equation (5) divides into two simplest ones:

$$p_x = p_b = 2\cos\psi_b \text{ and } \varphi_x = \varphi_b. \quad (6)$$

Of course, if we know these two parameters of impedance ratio anyone other desired impedance parameters can be easily calculated.

To balance the bridge we use variational method [28]. In this case we measure the initial bridge unbalance signal U_{n1} first. After that we provide the variation of the bridge balancing parameters (the angles ψ or φ), and measure the new unbalance signal U_{n2}. For certainty check, let's change the angle ψ, adding variation $\Delta\psi_v$ (change of the U_{n1} magnitude ρ by $\Delta\rho_v$). Following system of equations describes this process:

$$\rho_x e^{-j\varphi_x}|U_0| - \rho e^{-j\varphi}[U_0] = U_{n1}(Z_x + Z_0)/Z_0;$$
$$\rho_x e^{-j\varphi_x}|U_0| - (\rho + \Delta\rho_v)e^{-j\varphi}[U_0] = U_{n2}(Z_x + Z_0)/Z_0. \quad (7)$$

From (7) we find:

$$\frac{\rho_x}{\rho} e^{-j\Delta\varphi} = (1 - A\delta_v); \quad (8)$$

where: $A = \frac{U_{n1}}{U_{n2}-U_{n1}} = \left|\frac{U_{n1}}{U_{n2}-U_{n1}}\right| e^{-j\varphi_a} = |A| e^{-j\varphi_a};$

$$\delta_v = \frac{\cos(\psi + \Delta\psi_v)}{\cos\psi} - 1 \approx -\mathrm{tg}\psi \sin\Delta\psi_v.$$

Using Euler transformations for exponential functions equation (8) can be written by the following system of equations:

$$-\frac{\rho_x}{\rho}\sin\Delta\varphi = |A|\cdot\delta_v\cdot\sin\varphi_a;$$

$$\cos\Delta\varphi = \frac{\rho}{\rho_x}(1 - |A|\cdot\delta_v\cdot\cos\varphi_a). \quad (9)$$

Solving (9) we get formulas to calculate the distance $\delta\rho$ and $\Delta\varphi$ between the current bridge point (ψ, φ) and the point of the bridge balance (ψ_b, φ_b):

$$\delta\rho = -1 + \sqrt{1+B} \approx \delta_v|A|\cos\varphi_a;$$

$$\sin\Delta\varphi = -\delta_v|A|(1+\delta\rho)\sin\varphi_a; \quad (10)$$

where: $B = 2\delta_v \frac{|A|\cdot\cos\varphi_a}{(1-2\delta_v|A|(\cos\varphi_a - |A|\delta_v/2)} = \approx 2\delta_v|A|\cos\varphi_a.$

Using (10) we calculate the coordinates of the bridge balance point, enter them into synthesizers S_1 and S_2 and achieve the full bridge balance.

Two main factors determine the uncertainty δ_b of the bridge balance:

- uncertainty δ_{vv} of the VV measurement (its relative nonlinearity and sensitivity) which varies from 10^{-5} to 10^{-4};
- relative discreteness δ_d of the phase control.

Discreteness δ_d depends on the accuracy of the sinusoidal wave approximation, on the number of the steps on the period of the signal. It depends on the speed of the DACs, used in synthesizers, and lies in the range from 10^{-5} (on low frequencies) to 10^{-3} (on audio or higher frequencies).

Of course such uncertainty of the bridge balance is too big. Because of it, the balance procedure in our case consists of two steps:

1. On the first step the variation δ_v is high. It could consist, for example, in the change of the balancing voltage U_1 of 0 to its maximal value ($\sqrt{2}U_0$). The VV provides two measurements before and after the variation with minimal sensitivity S_{min}, and transfer these data to MC. Last one calculates values $\delta\rho$ and $\Delta\varphi$, enters these results in synthesizers S_{11} and S_{21} and change the voltage U_1 to its balancing value U_{1b}. If the uncertainty δ_{vv} of the VV measurement is $\delta_{vv} \leq \delta_d/2$, the uncertainty δ_b of the bridge unbalance will have, practically, the value δ_d.
2. On the second step MC increases the sensitivity S_{vv} of the VV to the value $S_{max} = S_{min}/\delta_d$ and varies the voltage U_1 by one unit δ_d of its discreteness. VV provides again two measurements of the unbalance signal as earlier. MC calculates by formulas (9) the new $\delta\rho$ and $\Delta\varphi$ values. PC digitally add these results to the data, written earlier in synthesizers S_{11} and S_{21} and uses these summed data to calculate the real value of the ratio $\frac{Z_x}{Z_0}$. The uncertainty δ_{be} of such equivalent bridge balancing and calculation of the ratio ${}^{Z_x}/_{Z_0}$ doesn't exceed $\delta_{be} \leq 2\delta_d\delta_{vv}$.

Let's assume that the δ_d is less than $1\cdot10^{-4}$ and the δ_{vv} is less than $1\cdot10^{-4}$. In this case the δ_{be} is less than $2\cdot10^{-8}$.

Bridge calibration procedure

The uncertainty, shown above, doesn't take into account the uncertainty of the synthesizers transfer coefficients. Last ones are rather big. To eliminate this uncertainty we provide bridge calibration. Let's consider one possible calibration procedure.

Let's perform balance equation. Additional signals U_{11} and U_{21} could be described by equations: $U_{11} = U_{11n} + \Delta U_{11} = U_{11n}(1 + \delta_{11})$ and $U_{21} = U_{21n} + \Delta U_{21} = U_{21n}(1 + \delta_{21})$ (see fig. 1). These signals have nominal values U_{11n} and U_{21n} and constant relative deviations δ_{11} and δ_{21} from nominal value. Using these formulas we could rewrite balance equation (3) into following equivalent form:

$$\frac{Z_x}{Z_0} = \frac{U_{11n}}{U_0}(1+\delta_{11}) + \frac{U_{21n}}{U_0}(1+\delta_{21}). \quad (11)$$

Here values δ_{11} and δ_{21} don't depend on the angles ψ and φ.

Calibration procedure determines values δ_{11} and δ_{21} and consists of two similar separate steps:

- calibration of the synthesizer S_{11};
- calibration of the synthesizer S_{21}.

On the first step of the calibration procedure we switch off the operation of the synthesizer S_{21} (for example, entering and maintaining zero control codes into this synthesizer). After that we set into synthesizer S_{11} the codes, corresponding to equality: $-U_{11} = U_0$ (see fig. 1).

The calibration circuit, which consists of the standards Z_1 and Z_2 ($Z_1 \approx Z_2$), is connected to the outputs of the synthesizer S_0 and the adder Σ through the switcher C_1 (see fig. 2). The switcher C_1 reverses the phase of the calibration circuit connection to the mentioned signal sources during the calibration process.

Calibration procedure uses variation and replacing methods [25, 28] and consists of the following stages.

1. *First stage*. The switcher C_2 connects the vector voltmeter to the output of the Z_1–Z_2 divider. Switcher C_1 remains in the initial position and the vector voltmeter measures the unbalance signal – U_{n1}.

2. *Second stage*. The MC varies the synthesizer S_{11} transfer coefficient on δ_d (one unit of discreteness). After that, the vector voltmeter measures the unbalance signal – U_{n2}.

3. *Third stage*. The MC reverses the switcher C_2 and the vector voltmeter measures the unbalance signal – U_{n3}.

The following system of equations describes these measurements:

$$U_0 - \frac{U_0 - U_0(1+\delta_{11})}{Z_1+Z_2} \cdot Z_1 - U_{n1} = 0;$$
$$U_0 - \frac{U_0 - U_0(1+\delta_{11}+\delta_v)}{Z_1+Z_2} \cdot Z_1 - U_{n2} = 0;$$
$$U_0 - \frac{U_0 - U_0(1+\delta_{11})}{Z_1+Z_2} \cdot Z_2 - U_{n3} = 0. \quad (12)$$

Neglecting the second order terms we get the next result:

$$\delta_{11} \approx \frac{\delta_v}{2} \cdot \frac{U_{n1}-U_{n3}}{U_{n2}-U_{n1}}. \quad (13)$$

So, using equation (13), we can find relative deviation δ_{11} of the synthesizer S_{11} transfer coefficient from nominal. This result does not depend on additive or multiplicative voltmeter errors. Its uncertainty depends only on the voltmeter nonlinearity and sensitivity.

On the second step of the calibration procedure we switch off the synthesizer S_{11}. After that we set into synthesizer S_{21} the codes, corresponding to the equality $U_0 = -U_{21n}$ (see fig. 1) and repeat the previously mentioned calibration procedure. In such way we get the value $\delta_{21} = \Delta U_{21}/U_0$.

To correct the result of the ratio Z_x/Z_0 measurement, the U_{11b} and U_{21b} have to be divided by (1+ δ_{11}) and (1+ δ_{21}) accordingly.

Bridge four terminal connection

Bridge, described above, accurately measures high impedance standards ratio with two terminal connection. For lower impedance measurements, bridge has to measure impedances using four terminal connections.

Four terminal connection in high potential part of the bridge

Structure of the appropriate bridge, using four terminal connection measurements, is shown in fig. 3 [29].

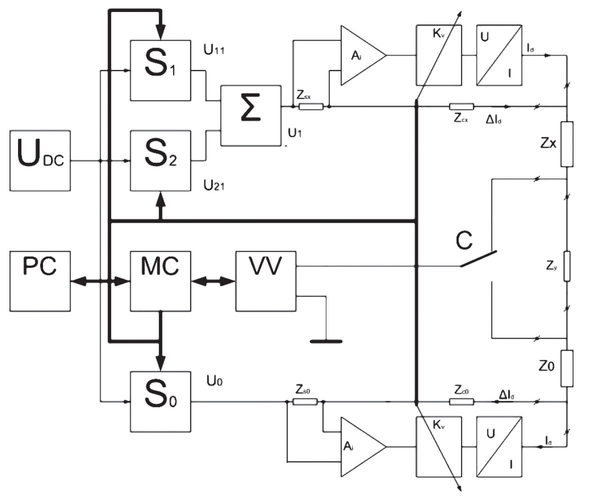

Fig. 3. Four terminal bridge diagram (without calibration divider)

Bridge contains two voltage sources U_0 (synthesizer S_0) and U_1 (synthesizers S_{11} and S_{21} and adder Σ). Magnitude of the voltage U_1 is controlled by phase changing. It is used for the bridge balance by the procedure, described above.

To compare the standards Z_0 and Z_x, we connect them to the voltage sources U_0 and U_1 by the potential cables, having impedances Z_{c0} and Z_{cx}. Impedance of the cable, which connects the standards Z_0 and Z_x ("Yoke") is equal to Z_y. The influence of these impedances on the result of measurement has to be eliminated.

To eliminate the influence of the cable impedances Z_{c0} and Z_{cx} on the result of measurement both hardware and algorithmic solutions are used.

Let's consider the bridge in fig. 3. In this bridge, the cable impedances Z_{cx} and Z_{c0} changes the view of the bridge balance equation (3) to the next form:

$$\frac{(Z_1+Z_{cx})}{Z_0+Z_{c0}} \approx \frac{Z_x}{Z_0}\left(1-\frac{Z_{c0}}{Z_0}\right) + \frac{Z_{cx}}{Z_0} = \frac{U_{1b}}{U_{0b}} = \mathrm{A}_0. \quad (14)$$

Following formulas describe the multiplicative $\delta(\delta_c)$ and additive $\Delta(\delta_c)$ components of the uncertainty δ_c, caused by the cable impedances Z_{cx} and Z_{c0}:

$$\delta(\delta_c) \approx \frac{Z_{co}}{Z_-};\ \Delta(\delta_c) \approx \frac{Z_{cx}}{Z_0}. \quad (15)$$

a) To decrease this uncertainty, we use in both bridge arms (see fig.3) the voltage/current transmitter with the transfer admittance Y_g, together with appropriate current sensors Z_s. Every such transmitter consists of the serially connected OpAmp A_i, variational divider K_v with transfer coefficient 1 or K_v and converter U/I. Converter U/I operates as current generator which, through the high potential current ports, supply the standards Z_x and Z_o with current I_d. Due to the feedback, only a little current ΔI_d flows through high voltage ports. Ratio of these currents is equal to $\Delta I_d / I_d = 1/\ 1 + Z_s \cdot Y_g$.

Due to this effect the equivalent values Z_{cxe} and Z_{coe} of the cable impedance $Z_{cx(0)}$ decreases in the same ratio, so that:

$$Z_{cxe} = \frac{Z_{cx}}{1+Z_s Y_g}; \qquad Z_{coe} = \frac{Z_{co}}{1+Z_s Y_g}. \quad (16)$$

The appropriate result of measurement in this case is described by the equation:

$$\frac{Z_x+Z_{cxe}}{Z_0+Z_{coe}} = A_0 \approx \frac{Z_x}{Z_0}\left(1+\frac{Z_{c0e}}{Z_0}\right)+\frac{Z_{cxe}}{Z_0}. \quad (17)$$

If the cable impedance $Z_c \le 0.1$ Ohm and the $Z_s Y_g \ge 5000$ (usual values for frequencies lower than units of kHz), measurement uncertainty $\delta_{cx(0)}$, caused by the cable impedances is lower than 10^{-7} for $Z_{x(0)} \ge 100$ Ohm.

But for the measurements of lower impedances (10 Ohm or less) this solution gives too big uncertainty.

Four terminal connection in high potential part of the bridge with variational correction

To decrease uncertainty in lower parts of the impedance range we sequentially vary the open loop amplification of $Z_s Y_g$ to $K_v Z_s Y_g$ in both bridge branches by dividers K_v and provide two additional bridge balances.

These two bridge balances are described by two equations:

$$\frac{z_x + z_{cxev}}{z_0 + z_{coe}} = A_1 \quad (18)$$

and

$$\frac{z_x + z_{cxe}}{z_0 + z_{coev}} = A_2 \quad (19)$$

where:

$$Z_{cxev} = \frac{Z_{cx}}{1+K_{vx} Z_s Y_g} \approx \frac{Z_{cx}}{K_{vx} Z_s Y_g};\ Z_{coev} = \frac{Z_{co}}{1+K_{v0} Z_s Y_g} \approx \frac{Z_{c0}}{K_{v0} Z_s Y_g}.$$

The system of equations (17), (18) and (19) gets us following formulas for ratios Z_{c0e}/Z_0 and Z_{cxe}/Z_1:

$$\frac{Z_{cxe}}{Z_1} = \left(1-\frac{A_1}{A_0}\right)\frac{K_{vx}}{\frac{A_1}{A_0}K_{vx}-1} \text{ and } \frac{Z_{c0e}}{Z_0} = \left(1-\frac{A_0}{A_2}\right)\frac{K_{v0}}{\frac{A_0}{A_2}K_{v0}-1}. \quad (20)$$

By substitution of the (20) in (17) we eliminate influence of the cable impedances Z_{c0} and Z_{c1} on the result of measurement:

$$\frac{Z_x}{Z_0} = A_0 \frac{1+(1-\frac{A_0}{A_2})\frac{K_{v0}}{1-\frac{A_0}{A_2}K_{v0}}}{1+(1-\frac{A_1}{A_0})\frac{K_{vx}}{1-\frac{A_1}{A_0}K_{vx}}}. \quad (21)$$

Additional analysis shows that we get maximal accuracy if $K_v = 0{,}5$.

Let's use the same value for K_{vx} and K_{v0}. In that case:

$$\frac{Z_x}{Z_o} \approx \frac{A_0}{1+\frac{A_1}{A_0}-\frac{A_0}{A_2}}. \quad (22)$$

Equation (22) shows that the uncertainty of measurement depends on the uncertainty of the variation and uncertainty of the equivalent bridge balancing. Let's that the cable impedance Z_c is lower than 0,1 Ohm, the open loop amplification $Z_s Y_g$ is higher than 5000 and the uncertainty of the variation δK_v is lower than 10^{-3}. In this case the measurement uncertainty, caused by the impedance of the potential cables on the range of measurement $Z_{1(0)} \ge 1$ Ohm, doesn't exceed 10^{-7}.

Four terminal connection in low potential part of the bridge

To eliminate the influence of the "Yoke" impedance Z_Y on the result of measurement we balance the bridge twice, connecting the *VV* sequentially to the low potential ports of the standards Z_1 and Z_o by the switcher S_{vv}. Two equations describe the results of these balances:

$$\frac{Z_x+Z_Y}{Z_0} = A_0;\quad \frac{Z_x}{Z_0+Z_Y} = A_3. \quad (23)$$

Solving system (23) we get equation (24) which fully eliminates influence of the "Yoke" impedance:

$$Z_x / Z_o = A_3 (1 + A_o) / (1 + A_3). \quad (24)$$

In real algorithm we provide five measurements of the appropriate unbalance signals, solve the common system of equations which describe these measurements and get exact result of measurement.

Four pair terminal connection

For accurate AC impedance measurement we have to eliminate AC interferences using four pair terminal

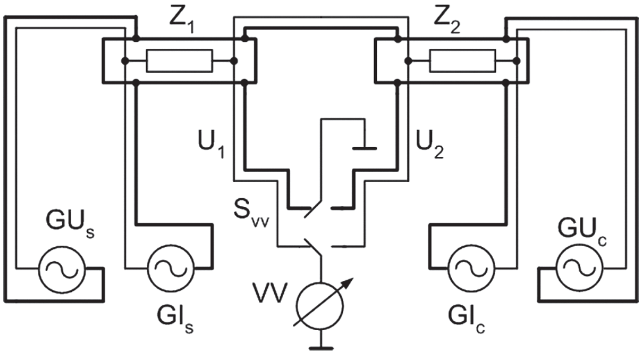

Fig. 4. Four pair terminal connection

connection of the standards being compared [8, 9, 30]. Unfortunately, we can not use classic equalizers (special current or voltage transformers) to get such connection on low frequencies.

Let's connect impedances being compared to the bridge voltage and current generators GU_s, GI_s, GU_c, GI_c and vector voltmeter *VV* using separate cables, as it is shows on figure 4 [31]. If the supply of these generators are fully separated, the *AC* currents, which flow through central wire and screen of every cable, will have the same values and opposite directions. This will satisfy requests for four pair terminal connection.

Usually all electronic current and voltage generators are supplied by the same main *DC* source, so that all their grounds are connected together. It creates additional currents, which flow through cables screens and violate the four pair terminal connection requests.

Development and implementation of the appropriate number of separated and properly protected *DC* supply sources for every *AC* current and voltage generators could resolve the problem. But it makes devise much more complex.

This is the reason why we use four quasi-separated *DC* sources shown on fig. 5.

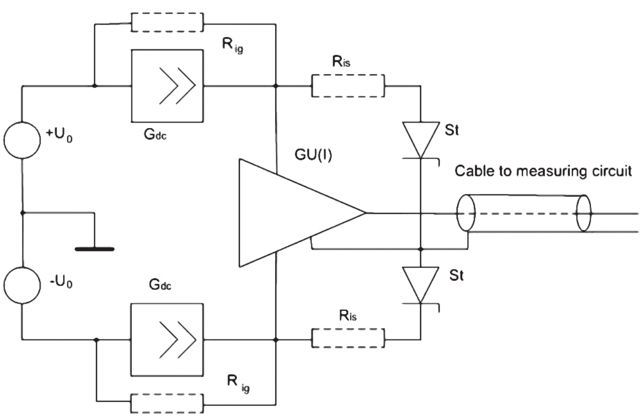

Fig. 5. Quasi-separated DC sources

Main *DC* source in our case supplies four quasi-separated *DC* sources. Every such source consists of the *DC* current generator G_{dc}, connected between main *DC* source and appropriate *AC* generator *GU*(*I*) which, in turn, is connected in parallel with *DC* voltage stabilizer *St*. Screen of the appropriate cable is connected to low potential points of the appropriate generator and *DC* voltage stabilizer.

Inequality of the currents in central wire and screen in every cable depends on the ratio of the internal resistance of the *DC* current generators and voltage stabilizers. Let's the internal resistance R_i of the *DC* current generator is more than 10^5 Ohm and internal resistance R_u of the *DC* voltage stabilizer is less than 10 Ohm (usual values). In this case only the little part of the generator output current will flow through main supply and, therefore, creates inequality of the currents of the cables central wire and screen. This relative current inequality δI will not exceed in our case value: $\delta I = R_u \,/\, R_i \le 10^{-4}$. It is enough to decrease the uncertainty, caused by non ideal four pair terminal connection, to values, less than 10^{-7} in whole range of impedances comparison. This inequality we test by classic method on the highest frequency of the frequency range, where this effect has most big influence on the uncertainty of measurement.

To get correct comparison of the drop of the voltage on the impedance being compared and appropriate *AC* voltage source (to measure correctly voltages on the low potential ports of both standards Z_1 and Z_2) both terminals of the *VV* are switched as it is shown on fig. 5. In this case electrical model of the bridge fully coincides to the system of equation (7).

Main uncertainty sources and their influence redusing

Uncertainty of the variation method

To get the result of measurement in described bridge we process the results of many independent measurements. Of course, it increases the common uncertainty of impedance measurement and, therefore, need appropriate analysis.

Let we'll analyze this uncertainty during high impedance measurements.

Whole uncertainty of measurement consists of the uncertainty of the separate bridge balance (formula (8)) and the calibration uncertainty (formula (13)).

a) Uncertainty of the separate bridge balance

Formula (8) shows that the uncertainty of the bridge balance measurement depends on the uncertainties ΔU_{n1} and ΔU_{n2} of the unbalance signals U_{n1} and U_{n2} measurement, uncertainty $\Delta\delta_{vb}$ of the variation δ_{vb} and on the instability δ_g of the voltages ratio U_1/U_0 during the time between two measurements.

Let $\Delta U_{n1} = \Delta U_{n2} = \Delta U_{nb}$, and $A_b\Delta\delta_{vb} \ll \Delta A_b\delta_{vb}$. These assumptions are valid because of we use the same VV in the same conditions of measurement and because of we implement variation using phase control.

In this case, using formula (7), we find the measurement uncertainty:

$$\Delta\left(\frac{Z_x}{Z_0}\right)_b = \delta_{vb}\,\delta U_{nb}\sqrt{1 + 2A_b(1 + A_b)} + \delta_g \quad (25)$$

where: $A_b = \frac{U_{n1}}{U_{n2}-U_{n1}}$ (see formula (8))

and $\delta U_{nb} = \frac{\Delta U_{nb}}{U_{n2}-U_{n1}}$.

b) Calibration uncertainty

Formula (13) shows the result of the calibration. Suppose, as earlier, that the uncertainties of all calibration measurements are the same and are equal to ΔU_{nc} and $A_c\Delta\delta_{vc} << \Delta A_c\delta_{vc}$. Using formula (12) we find:

$$\Delta\delta_{11} = \Delta\delta_{21} = \frac{\delta_{vc}}{\sqrt{2}}\delta U_{nc}\sqrt{1 + A_c + {A_c}^2} + \delta_g$$

and

$$\Delta\delta_1 = \delta_{vc}\delta U_{nc}\sqrt{1 + A_c + {A_c}^2} + \sqrt{2}\delta_g \qquad (26)$$

where: $A_c = \frac{U_{n1}-U_{n3}}{U_{n2}-U_{n1}}$ (see formula (13)),

δ_{vc} – variation during the calibration

and $\delta U_{nc} = \frac{\Delta U_{nc}}{U_{n2}-U_{n1}}$.

Whole uncertainty of the $\Delta\left(\frac{Z_x}{Z_o}\right)_c$ measurement, taking into account uncertainty of calibration, can be calculated by the formula:

$$\Delta\left(\frac{Z_x}{Z_o}\right)_c = \delta_v\, \delta U_n\sqrt{1 + 2A_b(1 + A_b) + (1 + A_c + {A_c}^2)} + \sqrt{3}\delta_g. \qquad (27)$$

Here we suppose that $\delta_{vc} = \delta_{vb} = \delta_v$.

Formulas (25)–(27) show that the uncertainty of measurement quickly increases when values A_b and A_c increase. Because of it the better result we will get if the bridge will be matched so, that $A_b \le 1$ and $A_c \le 1$.

Let $|A_{bmax}| = |A_{cmax}| = 1$. In this case:

$$\Delta\left(\frac{Z_x}{Z_0}\right)_{cmax} = \sqrt{8}\delta_v\delta U_n + \sqrt{3}\delta_g. \qquad (28)$$

We have got last formulas supposing that instability of the generators voltages ratio during the measurement and during the calibration is described by linear function. For more exact calculations the spectrum of this function has to be taken into account.

Formula (28) shows that:

δU_n determines the uncertainty of measurement with low weight $\sqrt{8}\delta_v$ (usually $10^{-5} \le \delta_v \le 10^{-3}$);

δ_g determines the uncertainty of measurement with big weight $\sqrt{3}$.

Let's consider this instability.

Instability of the generated voltages depends on two factors: instability of the used OpAmp gain and temperature instability of the used *DAC*.

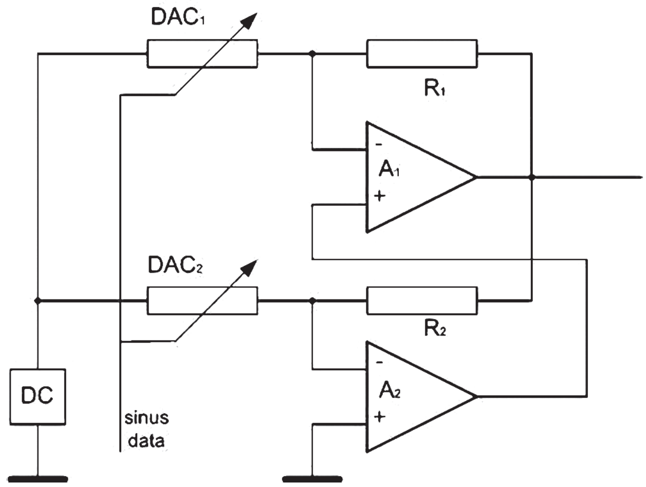

Fig. 6. Generator's iterative structure

To decrease the influence of the OpAmp gain on the voltage instability, voltage generators have two-cannel iterative structure (see fig. 5) [32].

First channel consists of OpAmp A_1 and DAC_1. This channel generates main part of the signal. The DAC_2 of the second cannel forms the small signal, proportional to the error of the first channel and, through OpAmp A_2, add it to the pozitive input of the first channel. In this structure uncertainty, caused by limited values of the amplifiers gains can be estimated by formula $\delta_g = \frac{1}{(K_1\beta_1)(K_2\beta_2)}$, where $(K_1\beta_1)$ and $(K_2\beta_2)$ are open loop gains of the first and second channels. Let we will suppose that these values are the same for both channels and doesn't exceed 5000. In this case δ_g doesn't exceed $4\cdot10^{-8}$ and its short term instability during two measurement doesn't exceed units of 10^{-9}.

We use in both voltage generators *DAC* with temperature coefficient better than 2 ppm/°C. To decrease the *DAC* temperature instability on the result of comparison, the DAC_2 of the second channels are set into passive thermostat, so that *DAC* temperature instability during the measurement (less than 1 min.) doesn't exceed 0,001–0,002 °C. In such way the generators voltage instability during the measurement doesn't exceed 5–10 bpm.

Experimental results

Experimental investigations of the described bridge have shown that on the main part of the range of impedance comparison the uncertainty of comparison doesn't exceed of 1 ppm and sensitivity isn't worse than $0{,}3\cdot10^{-8}$. Two bit phase divider was used in quadrature bridge, tested in PTB. Comparisons of the capacitive and resistive standards by this bridge have shown that uncertainty of this bridge doesn't exceed 0,4 ppm [33].

Conclusion

1. Bridges with phase control can measure the impedance ratios with uncertainty better than 1 ppm.

This uncertainty is restricted by instability of the synthesizer parameters during the time of measurement and their phase noise.

2. Calibration procedure reduces the influence of the synthesizer's uncertainty on the result of measurement.

3. Automatic variational bridge balance significantly reduces the balance time and in such way decrease the influence of the synthesizer instability on the result of measurement.

4. Automatic variational correction widens the range of impedance ratio measurement.

5. Modern components make possible development of the bridges with phase control, which have very small dimensions and price.

6. Phase control is the way for creation of the accurate AC bridges for impedance measurements as integral component.

7. In high frequency range there is the limitation, caused by operation speed and number of digits in synthesizers. Last one determines only discreteness of the bridge balancing.

Acknowledgements. The authors are very grateful to Dr. Y. Wang, and Dr. A. Koffman (NIST, USA), Dr. H. Bachmair and Dr. M. Klonz (PTB) for their constant support and very useful advices during the development of these ideas.

Reference

1. *Hall H.P.* A History of Z measurement, 64 pp., www.ietlabs.com/pdf/GenRad_History/A_History_of_Z_Measurement.pdf), 2007
2. *Blumlein A.D.* Alternating Bridge circuits., British Patent No. 323,037, The Illustrated Official Journal of Patents, pp. 7727-772812, Feb. 1930.
3. *Thompson A.M.* The Precise Measurement of Small Capacitances, IRE Trans Instr. 1958.
4. *Jeffery A.M., Shields J., Shields S., Lee L.H.* New Multi-frequency Bridge at NIST, BNM-LCIE, pp. G1-G37, 1998.
5. *Small G.* Two-terminal-port AC bridges at NML, BNM-LCIE, pp. B1-B18, 1998.
6. *Delahaye F.* AC-bridges at BIMP. BNM-LCIE, pp.C1-C6, 1998.
7. Трансформаторные измерительные мосты / под ред. К.Б. Карандеева. – М.: Энергия, 1970. – 280 с.
8. *Kibble B.P., Rayner G.H.* Coaxial AC Bridges., Adam Hilger Ltd., Bristol, p.203 p. 1984.
9. *Awan Shakil, Kibble Bryan, Schurr Jurgen.* Coaxial Electrical Circuits for Interference-Free Measurements, The Institution of Engineering and Technology, London, United Kingdom, 321 pp., 2011.
10. *Thompson A.M.* An absolute determination of resistance, based on calculable standard of capacitance., Metrologia, Vol. 4, № 1б, pp. 1–7, January, 1969.
11. *Trapon G., Thevenot O., Lacueille J.C., Poirier. W.* Determination of the von Klitzing constant RK in terms of the BNM calculable capacitor – fifteen years of investigations", Metrologia, Volume 40, Issue 4, pp. 159-171, August 2003.
12. *Wood B., Cote M.* AC Bridges for the R-C Chain. BNM-LCIE, pp. E1-E20, 1998.
13. *Chua S.W., Kibble B.P., Hartland A.* Comparison of Capacitance with AC Quantized Hall Resistance. Conference on Precision Electromagnetic Measurements, Washington DC, USA, 6-10, pp. 418-419, July, 1998.
14. *Trapon G., Thevenot O., Lacueille J.C., Poirier W., Fhimia H., Geneves G.* Progress in linking of the Farad and the Rk to the SI Units at BNM, LCIE, CPEM 2000, Conference Digest, pp. 214-215, 2000.
15. *Callegaro L., D'Elia, Bava E., Galzerano, Svelto C.* Polyphase Synthesizer for Unlike-Impedance Intercomparison System. CPEM2002. Conference Digest., pp. 176-177, 2002.
16. *Corney A.* Digital generator assisted impedance bridge, IEEE Trans. Instrum. Meas., vol. 52, no. 2, pp. 388–391, 2003.
17. *Bachmair H., Vollmert R.* Comparison of admittances by means of a digital double-sine wave generator, IEEE Trans. Instrum. Meas., vol. 29, no. 4, pp. 370–372, 1980.
18. *Cabiati F. and Bosco G. C.* LC comparison system based on a two-phase generator, IEEE Trans. Electron Devices, vol. 34, no. 2, pp. 344–349, 1985.
19. *Ramm G.* Impedance measuring device based on an ac potentiometer, IEEE Trans. Instrum. Meas., vol. 34, no. 2, pp. 341–344, 1985.
20. *Muciek A.* Digital impedance bridge based on a two-phase generator, IEEE Trans. Instrum. Meas., vol. 46, no. 2, pp. 467–470, 1997.
21. *Callegaro L., D'Elia V., Trinchera B.* Realization of the Farad from the DC quantum Hall effect with digitally assisted impedance bridges, Metrologia, 47, 464, 2010.
22. *Overney F. and Jeanneret B.* Sampling based RLC bridge, Proc. CPEM Dig., pp. 400–401, 2010.
23. *Overney F. and Jeanneret B.* RLC Bridge based on an automated synchronous sampling system, IEEE Trans on Inst., vol. 60, 7, 2393-2398. 2011.
24. *Surdu M.N., Lameko A.L., Karpov I.V., Kinard J., Koffman A.* Theoretical basis of variational quadrature bridge design of alternative current, Measurement Techniques, Moscow., № 10., 58–64 pp., 2006.
25. *Surdu M., Surdu D., Koffman A.* Precision universal AC bridges with phase controlled dividers, CPEM-2010, Korea, 2010.

26. *Сурду М., Сурду Д.* Спосіб формування напруг із заданим відношенням. Патент України № 102277, опубл. 25.06.2013, Б.и. №12.
27. *Surdu M., Surdu D.* Phase control as basis for precise impedance bridge microminiaturization, XVIII IMEKO TC4 Symposium and IX Semetro Digest, Natal, 2011.
28. *Гриневич Ф. В., Сурду М. Н.* Высокоточные вариационные измерительные системы переменного тока. – Киев: Наукова Думка, 1989. – 209 с.
29. *Surdu M., Surdu D.* Wide Range Bridge-Comparator for Accurate Impedance Measurements on Audio- and Low Frequencies, CPEM-2014, Digest, Rio-da-Janeiro, 23-26 August, 2014.
30. *Tompson A.M.* The precise Measurement of Small Capacitances, IRE Trans. Instr., Volume: I-7, Issue: 3, 245–253 pp., 1958.
31. *Cabiati F., d'Ella V.* A new architecture for high-accurate admittance measuring system, Conference on Precision Electromagnetic measurements, CPEM2002, 178-179 pp. 2002.
32. *Осмоловский П.Ф.* Итерационные многоканальные системы автоматического управления. — М.: Советское радио, 1969. — 256 с.
33. *Surdu M., Lameko A., Karpov I., Koffman A., Kinard J., Klonz M., Melcher J., Tarlowsky A.* Complex of bridge comparators for impedance unit traceability and impedance measurements // Digest of 2006 Conference on Precision Electromagnetic Measurement. – Torino, Italy, 2006. – P. 520–521.